8

Brief Overview of the Younger Dryas Cosmic Impact Datum Layer 12,800 Years Ago and Its Archaeological Utility

malcolm a. lecompte, a. victor adedeji, james p. kennett, ted e. bunch, wendy s. wolbach, and allen west

Firestone et al. (2007) proposed that a major cosmic impact event occurred 12,800 ± 150 calendar years ago (cal B.P.), with major environmental, climatic, biotic, and human consequences. The hypothesized cause is cosmic airburst/impacts, a term referring to atmospheric collisions by extraterrestrial bodies, typically producing explosive, aerial disintegrations, sometimes along with small crater-forming ground impacts. This scenario is part of the Younger Dryas (YD) impact hypothesis that is supported by an increasing body of evidence across multiple continents. As discussed in chapter 9 in this volume, this impact is proposed to have triggered or contributed to the abrupt cooling of the Younger Dryas episode and caused major environmental disruptions. These changes may have also contributed to major extinctions of Pleistocene megafauna and to significant human population declines and cultural changes over broad areas of the Northern Hemisphere (Anderson et al. 2011; Firestone et al. 2007; Kennett et al. 2008; Kennett et al. 2015; Wittke et al. 2013).

The YD impact hypothesis originated from observations of abundance peaks in a variable assemblage of high-temperature, impact-related materials, called proxies, which are found in the Younger Dryas Boundary layer (YDB), a sedimentary stratum typically a few centimeters in thickness (Firestone et al. 2007). Because these proxies have been extensively described and discussed in detail elsewhere, we provide only an overview here. Table 8.1 is a brief, non-exhaustive list of YDB impact-related proxy

Table 8.1. Contributions Related to YDB Proxy Data

Proxy	Proponents	Positive	Negative
Cosmic impact **spherules**	***Firestone et al. 2007***; Kennett et al. 2008; ***Israde et al. 2012***; Bunch et al. 2012; Wittke et al. 2013	Mahaney et al. 2010; Fayek et al. 2012; ***LeCompte et al. 2012***; Wu et al. 2013	Surovell et al. 2009; Pinter et al. 2011; Pigati et al. 2012
Meltglass (scoria-like **objects)**	***Bunch et al. 2012***; Wittke et al. 2013	Mahaney et al. 2010; Fayek et al. 2012; Wu et al. 2013	—
Nanodiamonds	Firestone et al. 2007; Kennett, Kennett, West, Mercer et al. 2009; Kennett, Kennet, A. West, G. J. West 2009b; Kurbatov et al. 2010; Israde et al. 2012; ***Kinzie et al. 2014***	Baker et al. 2008; Tian et al. 2011; Bement et al. 2014	Daulton et al. 2010; Pinter et al. 2011; van Hoesel et al. 2012
Anomalous geochemistry	***Firestone et al. 2007***; Kennett et al. 2008	Beets et al. 2008; Haynes et al. 2010; Andronikov et al. 2011, 2014; LeCompte et al. 2012; Petaev et al. 2013; Wu et al. 2013	Paquay et al. 2009; Pinter et al. 2011; Pigati et al. 2012
Aciniform carbon, carbon spherules, glass-like carbon, charcoal	***Firestone et al. 2007;*** Kennett et al. 2008; ***Israde et al. 2012***	Baker et al. 2008; Mahaney et al. 2010	Scott et al. 2010; Pinter et al. 2011; van Hoesel et al. 2012
Megafaunal extinctions	Firestone et al. 2007; Kennett et al. 2008; Anderson et al. 2011	—	—
Human population changes	Firestone et al. 2007; Kennett et al. 2008; Anderson et al. 2011	—	—

Note: Bold, italicized references contain detailed proxy extraction and analytical protocols.

studies, both by those who reported finding them and others with negative findings. In addition, those contributions providing the extraction and analytical protocols are noted. Although most independent investigations attributed the proxies to a cosmic impact event, some offered alternate explanations (e.g., Haynes et al. 2010; Tian et al. 2011). The studies reporting negative results did not use rigorous dating methods or did not follow the

requisite analytical protocol, for example, by not performing crucial analyses using scanning electron microscopy (SEM) and electron diffraction spectroscopy (EDS).

The primary purpose of this chapter is to offer a brief overview of the characteristics, origin, and distribution of the various impact-related proxies that can exhibit peak abundances in the YDB layer, thus allowing its identification as a chronostratigraphic datum that coincides with the YDB cosmic impact event. These include magnetic and glassy impact-related spherules, high-temperature minerals and meltglass, nanodiamonds, carbon spherules, aciniform carbon, platinum, osmium, iridium, and other elements at anomalous concentrations.

The YDB layer has been identified widely in 30 stratigraphic sections in 12 countries on four continents and has a modeled age range of 12,835–12,735 cal B.P. at 95 percent probability (Kennett et al. 2015). The widespread distribution of this now well-dated, synchronous layer makes it of great value as a datum for stratigraphic correlation over wide areas and for chronological underpinning of late Quaternary sequences, including those of interest to archeologists. The YDB layer has been documented in three sites in the U.S. Southeast, including the archeologically important site at Topper, South Carolina (Firestone et al. 2007; Goodyear and Steffy 2003; Kinzie et al. 2014; LeCompte et al. 2012; Waters et al. 2009; Wittke et al. 2013) and should be found in other sites with sediments that span the Younger Dryas onset.

Based on independent dating, the Younger Dryas onset (and hence, the YDB layer) had been already identified in time-series samples collected from stratigraphic sections at many locations. At all sites, cosmic impact-related proxies are generally present in trace quantities and/or as small particles, ranging in size from nanometers to several centimeters. Because of this, quantitatively describing their stratigraphic distribution often requires demanding, labor-intensive analyses. Hence, sampling protocols need to be guided by available age and sedimentary data within a paleontological and archeological context, when possible. The onset of the Younger Dryas episode is often well marked by distinct lithological changes and evidence for environmental degradation; it is synchronous with the upper biostratigraphic limits of many extinct taxa of late Pleistocene megafauna and/or artifacts of the Clovis culture. Prior knowledge of this stratigraphy has often been valuable in guiding sampling for time-series analyses of proxies in stratigraphic sections.

Identification of the YDB Layer

Primary Impact-Related Proxies

The materials described in this section (i.e., primary impact-related proxies) include those that were either directly produced or directly altered by a YDB impact event, generally due to very high temperatures but also to high pressures and low-oxygen conditions associated with a cosmic impact.

Spherules (Iron-Rich and Silica-Rich)

Characteristics

YDB spherules are mostly black or brown in color, although a few are red, blue, green, gray, tan, or white, ranging in clarity from opaque to transparent (Wittke et al. 2013). Although the diameters of spherules range from 5 μm to 5.5 mm, 80 percent of them have diameters of ≤55 μm (avg. 135 μm; median 30 μm) (Figure 8.1A-B). Most spherules (>95 percent) are rounded, and the remainder appear as ovoids, aerodynamically shaped teardrops, or fused clusters of one or more spherules. Concentrations in the YDB layer range from 5 to 4,900 spherules/kg, averaging 955/kg (median: 388/kg) (Wittke et al. 2013). The typical composition of YDB spherules is distributed across a continuum from pure iron (FeO) to pure silica (SiO2); FeO ranged from 0 to 100 percent, averaging 44.9 wt percent ; SiO2 ranged from 0 to 100 percent and averaged 30.9 wt percent. The abundances of a third oxide, Al2O3, ranged from 0 to 65 percent, averaging 12.2 wt percent. Ten other oxides collectively constituted < 5 wt percent of the total. A small percentage of spherules contain osmium and rare earth elements (lanthanum, cerium), ranging from < 1 wt percent to ≈40 wt percent in a few cases (LeCompte et al. 2012; Wu et al. 2013).

The presence of high-temperature melted minerals in Fe-rich spherules indicates that minimum formation temperatures were elevated. For example, titanomagnetite melts at ≈1,400 °C; schreibersite at ≈1,400 °C; magnetite at ≈1,550 °C; hercynite at ≈1,700 °C; rutile at ≈1,840 °C; and suessite at ≈2,300 °C (Bunch et al. 2012; Wu et al. 2013). These melting points can be slightly lower, depending upon the presence of suitable fluxing agents. Glassy spherules also often were found to contain high-temperature minerals, including wollastonite, with a melting point of ≈1,500 °C; corundum, mullite and sillimanite at ≈1,800 °C; and lechatelierite at ≈1,720 °C.

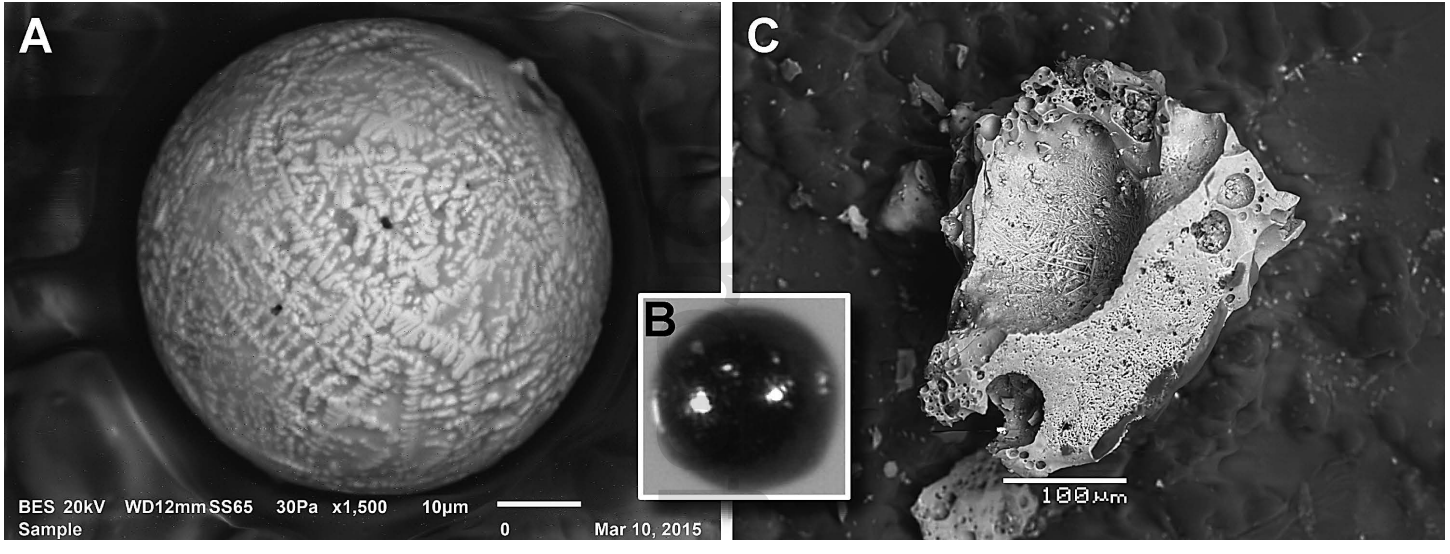

Figure 8.1. (A) SEM image of Fe-rich YDB spherule from Glacial Lake Hind, Manitoba, Canada, showing characteristic dendritic surface pattern. (B) Photomicrograph of 60-µm-wide, Fe-rich spherule from Lake Hind. (C) SEM image of YDB melt-glass from Newtonville, New Jersey, showing vesicular structure resulting from bubbling in molten state.

Distribution

Based on evidence from 27 YDB sites, an estimated 10 million tonnes of melted spherulitic objects are distributed across ≈50 million square kilometers of North and South America, Europe, and Asia (Wittke et al. 2013). They are present in high abundances only in the YDB layer and closely adjacent strata. Workers have also observed abundant unmelted, authigenic framboidal spherules that tend to peak in or near the YDB layer, and thus appear to be secondarily related, perhaps because environmental degradation created anoxic conditions that favored framboidal growth (Wittke et al. 2013).

Inconsistent Origins

(1) Primary cosmic origin: Fe-rich micrometeorites and cosmic spherules nearly always contain high abundances of nickel, with a range of 5–25 wt percent, averaging 10 wt percent (Wittke et al. 2013). In contrast, YDB spherules are depleted in nickel, having an average concentration of .1 wt, with a range of 0–2 wt percent. For Si-rich cosmic microspherules and micrometeorites, more than 98 percent are enriched in MgO at >10 wt percent, averaging 29 percent, with a range of 1–55 percent, whereas ≈98.8 percent of YDB spherules contain < 10 percent MgO (Wittke et al. 2013). These results indicate that very few YDB spherules are cosmic in origin, and instead, their composition matches that of melted terrestrial material. In addition, the high concentrations of YDB spherules in sediments are consistent with that of the Cretaceous–Paleogene (K-Pg) impact but are far higher than found in polar ice (Wittke et al. 2013 and references therein). One study of cosmic influx in Antarctic ice found an average of only one spherule in each 67 kg of ice (or .014 spherules/kg), whereas the average number of spherules in YDB sediment is 955 avg. spherules/kg (Wittke et al. 2013). (2) Anthropogenic origin: fly ash spherules, a common anthropogenic contaminant, have been deposited only since the beginning of the Industrial Revolution, and hence, their distribution is typically restricted to sediment depths of less than ≈20 cm from the ground surface. They form at temperatures of <1,400 °C, well below 1,800 °C, the melting point of many common minerals found in YDB spherules. Unlike fly ash, YDB spherules are typically buried deeper than anthropogenic spherules, at an average depth of 2.5 m (max: 15 m. (3) Authigenic origin: this process can be rejected because YDB spherules possess surface morphology,

visible only under SEM examination, that indicates incomplete crystal formation. Such features are evidence that they were melted and then rapidly quenched, unlike authigenic spherules, which are unmelted and crystallize slowly over a long period. (4) Volcanism: compared to volcanic spherules, YDB spherules average 8× higher in Cr, 11× higher in K, 3× lower in Mg, and 2× lower in Na, showing that they are geochemically dissimilar (Wittke et al 2013). In addition, volcanic spherules are invariably Si-rich, without high concentrations of Fe, as is found in many YDB spherules. (5) Lightning: measurements of remanent magnetism indicate that YDB spherules cooled rapidly in Earth's ambient magnetic field (Wittke et al. 2013). This eliminates the possibility that YDB spherules formed by lightning, which generates a strong magnetic field that can be easily detected in lightning-melted materials (Nabelek et al. 2013).

Impact-Related Origin

The shapes, composition, and surface textures of most YDB spherules are similar to those formed in the Tunguska airburst in 1908, the Australasian Tektite Field at ≈680 ka, Meteor Crater at ≈50 ka, the Chesapeake Bay impact at ≈35 Ma, and the K-Pg impact ≈65 Ma (Wittke et al. 2013). After eliminating all other known possibilities, a cosmic impact is the only remaining plausible explanation for high-temperature–quenched YDB spherules.

Formation Mechanism

Based on all available evidence, YDB spherules formed when high-temperature, hypervelocity jets descended to the ground from atmospheric explosions and melted terrestrial sediment, whether located on land, in glacial ice as detritus, or as oceanic sediments. Following formation, the rising impact plume(s) dispersed the spherules into the atmosphere and distributed them widely across multiple continents.

High-Temperature, Melted Silica-Rich Glass

Characteristics

Found at six sites in North and South America and Asia, YDB meltglass, also called scoria-like glass, exhibits a wide range of colors: black, brown, red, blue, green, gray, tan, and/or white, ranging in clarity from opaque to transparent (Bunch et al. 2012). Meltglass shapes range from small, angular,

glassy, shardlike particles to large masses of highly vesiculated glass. Sizes range in diameter from ≈300 μm to 11.75 mm, averaging 2.6 mm (Figure 8.1C). Although meltglass is generally enriched in silica, it exhibits a wide range in composition: FeO ranges from 0 to 82 wt percent, averaging 12 wt percent; SiO2 from 1 to 100 wt percent, averaging 55 wt percent; and Al2O3 from 0 to 65 wt percent, averaging 13 wt percents. Some small glass inclusions had high percentages of other important minerals: up to 37 wt percent of P2O5; 38 wt percent of NiO; 41 wt percent of MgO; 49 wt percent of SO3; and 60 percent of Cr2O3. YDB meltglass also contains some of the same high-temperature, melted minerals found in the spherules. For example, titanomagnetite melts at ≈1,400 °C, schreibersite at ≈1,400 °C, wollastonite at ≈1,500 °C, magnetite at ≈1,550 °C, hercynite at ≈1,700 °C, corundum at ≈1,800 °C, mullite at ≈1,800 °C, sillimanite at ≈1,800 °C, rutile at ≈1,840 °C, lechatelierite at ≈2,200 °C, and suessite at ≈2,300 °C (Bunch et al. 2012; Wu et al. 2013).

Distribution

Silica-rich YDB meltglass has been found in the United States (Arizona, Pennsylvania, New Jersey, New York, and South Carolina), as well as in Venezuela and northern Syria, an area spanning ≈50 million square kilometers (Bunch et al. 2012; Fayek et al. 2012; Firestone et al. 2007; Kinzie et al. 2014; Mahaney et al. 2010; Wittke et al. 2013). It has been found in high abundances only in the YDB layer and closely adjacent strata. In some sections investigated, small amounts of meltglass have been reworked upward and downward from the YDB layer by natural sedimentary and biogenic processes (Bunch et al. 2012).

Inconsistent Origins

Bunch et al. (2012) compared and contrasted potential origins of YDB meltglass and eliminated the following possibilities: (1) Cosmic origin: results indicate >90 percent of YDB high-temperature meltglass and spherules are geochemically dissimilar to cosmic-derived materials. (2) Anthropogenic origin: more than 75 percent of YDB objects have compositions different from anthropogenic objects, rejecting anthropogenesis as a potential origin. (3) Authigenic origin: this can be rejected because meltglass was once molten, by definition, unlike unmelted authigenic material. (4) Volcanic origin: approximately 85 percent of YDB objects are compositionally distinct from volcanic material, and furthermore, the YDB layer at all sites

contains no volcanic ash and tephra, thus refuting this origin. (5) Origin by lightning: studies of remanent magnetism indicate that YDB meltglass could not have formed by lightning (Nabelek et al. 2013).

Impact-Related Origin

The shapes, composition, and surface textures of YDB meltglass are similar or identical to meltglass formed in the Tunguska airburst, the Australasian Tektite Field, Meteor Crater, and other existing impact craters (Bunch et al 2012).

Formation Mechanism

YDB meltglass composition is terrestrial (Bunch et al. 2012), consistent with having formed as ejecta that contained little or no impactor material. During the impact, molten glass would have been ejected into the atmosphere when the high-temperature, hypervelocity airburst jet and/or the impactor reached the ground, forming a shallow crater. Because 95 percent of ejecta travels less than 5 crater radii, most ejected glass would have fallen out rapidly near the area of impact (Bunch et al. 2012 and references therein). However, some meltglass may have been distributed over greater distances, as occurred with the Australasian tektite field that covers ≈10 percent of the planet, and for which no crater has been found (Bunch et al. 2012 and references therein). Remanent magnetic measurements and high formation temperatures (≈1,500 to 2,200 °C) *rule out formation mechanisms other than cosmic impact.*

Nanodiamonds

Characteristics

Twenty-one YDB sites on three continents contain multiple polytypes of nanodiamonds, including cubic diamonds, lonsdaleite-like crystals, and diamond-like carbon nanoparticles called n-diamond and i-carbon (Kinzie et al. 2014). Typical shapes are spherical to ovoid, with sizes ranging from 2 to 10 nm, although a few YDB nanodiamonds are up to 2.9 μm in diameter (Figure 8.2A). YDB nanodiamond concentrations in bulk sediment ranged from ≈60 to 500 ppb (avg: 200 ppb), and in fire-related YDB carbon spherules (discussed below), they ranged from ≈10 to 3900 ppb (avg: ≈750 ppb) (Kinzie et al. 2014). After extraction, the identification and characterization

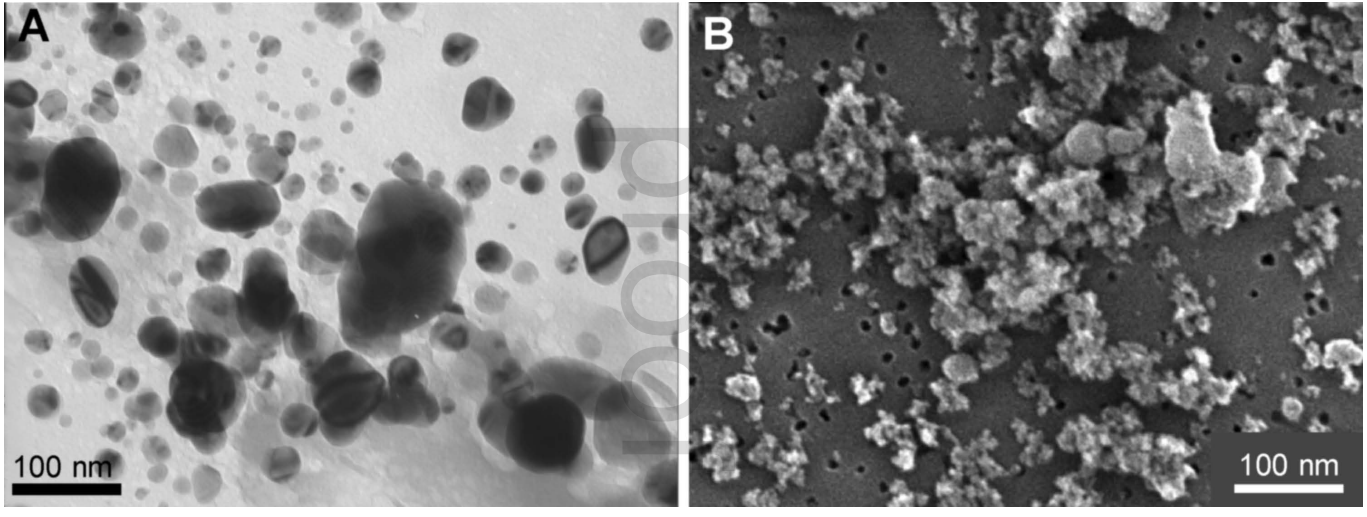

Figure 8.2. (A) TEM image of YDB nanodiamonds extracted from bulk sediments from Murray Springs, Arizona. (B) SEM image of aciniform carbon also from YDB bulk sediment at Murray Springs.

of YDB nanodiamonds requires high-resolution transmission electron microscopy (TEM), which is difficult and labor intensive.

Distribution

YDB abundance peaks in nanodiamonds have been reported for 24 dated stratigraphic sections in 10 countries across three continents, the same area as for YDB impact-related spherules (Kinzie et al. 2014). Peak abundances in nanodiamonds were exhibited at every YDB site tested.

Inconsistent Origins

(1) Cosmic origin: nanodiamonds are present in some cosmic dust particles and meteorites (Kinzie et al. 2014). However, based on carbon and nitrogen isotopic ratios (δ13C and δ15N), YDB nanodiamonds are not of cosmic origin (Israde et al. 2012; Kinzie et al. 2014; Tian et al. 2011), meaning that they did not arrive in micrometeorites or cosmic dust and were not derived from the impactor itself. (2) Anthropogenic origin: outside of the laboratory, modern high-energy explosives are the only known, widespread anthropogenic process capable of producing large numbers of nanodiamonds. However, that process can be rejected, because YDB nanodiamonds are widely distributed on three continents and deeply buried up to 4 m, ruling out formation in modern times. (3) Authigenic origin: no known or plausible mechanisms form nanodiamonds authigenically. (4) Volcanic origin: cubic diamonds do occur rarely in terrestrial deposits, such as mantle-derived kimberlite pipes. However, such diamonds are not found in any known, non-impact-related geological column that is associated with coeval peaks in impact-related proxies. Furthermore, such diamonds are always associated with geochemically distinctive mantle-derived rocks, which are absent at all YDB sites. (5) Origin by wildfires: based on more than a century of laboratory experiments, there is no evidence that nanodiamonds can be produced in wildfires, or by any other natural, terrestrial conditions on Earth's surface. If nanodiamonds could be produced in natural fires, they should be common and ubiquitous in sediments of all ages, but instead, they range from nonexistent to extraordinarily rare, being found in high abundances only in known or proposed impact-related sedimentary layers (Bement et al. 2014; Kinzie et al. 2014; Tian et al. 2011). (6) Origin by lightning: there are no confirmed mechanisms for nanodiamond production through lightning.

Impact-Related Origin

Nanodiamonds are commonly associated with known impact events, including the K-Pg impact at 65 Ma and with the Tunguska airburst over Siberia in 1908, to which they are morphologically and compositionally similar. The δ13C and δ15N ratios indicate YDB nanodiamonds were produced from terrestrial carbon, as is the case for all known impact-related nanodiamonds.

Formation Mechanism

It was proposed that K-Pg nanodiamonds formed by carbon vapor deposition (CVD) when the impactor collided with carbon-rich limestone strata (Kinzie et al. 2014 and references therein). Kinzie et al. (2014) discussed several lines of evidence suggesting that YDB nanodiamonds may have formed within the impact cloud by CVD. This mechanism requires elemental carbon vapor and low-oxygen atmospheric conditions, both of which would be present in an impact fireball (Wen et al. 2007) but do not occur naturally on Earth. In support of CVD, Kinzie et al. (2014) reported experiments demonstrating that nanodiamond formation requires anoxia combined with elevated temperatures of 1,000 to 1,200 °C. These conditions mirror those associated with cosmic impact but do not result from any other natural mechanism.

Geochemical Enrichments

Characteristics

Anomalous geochemical concentrations have been found in the YDB layer at 27 YDB sites, using electron diffraction spectroscopy (EDS), X-ray fluorescence spectroscopy (XRF), and instrumental neutron activation analysis (INAA) (Firestone et al. 2007). Anomalous concentrations in YDB sediments and a Younger Dryas–age Greenland ice core were observed for nickel, cobalt, chromium, rare earth elements (e.g., lanthanum and cerium), and/or platinum group elements (e.g., iridium, platinum, and osmium) (Andronikov et al. 2015; Bunch et al. 2012; Firestone et al. 2007; LeCompte et al. 2012; Petaev et al. 2013; Wittke et al. 2013; Wu et al. 2013). At 23 YDB sites on four continents, these anomalous concentrations peak only in the YDB layer and are at normal crustal abundances in sediments above and below the YDB layer.

Distribution

One or more geochemical anomalies are present in the YDB layer dating to 12,800 ± 150 cal B.P. at ≈27 sites examined across four continents, spanning ≈50 million km2.

Impact-Related Origin

The above anomalous elements in the YDB layer are known to be highly enriched in asteroids and are proposed to be enriched in comets (Firestone et al. 2007). The fact that their concentrations are anomalously high in the YDB layer at so many widely distributed sites supports a cosmic impact origin, rather than from unknown local elemental sources. The elemental enrichments could have resulted from two impact-related processes. First, these high concentrations could represent remnants of the vaporized impactor itself. Second, they could result from enriched target rocks ejected by impact(s) and widely distributed through the atmosphere.

Secondary Impact-Related Proxies

Fire-related: four kinds of material that result from high-temperature biomass burning have been found in peak abundances in the YDB layer across four continents. These are aciniform carbon, carbon spherules (with and without nanodiamonds), glass-like carbon (with and without nanodiamonds), and charcoal. A comparison of their relative abundances in the YDB layer compared with background concentrations provides evidence for an increase in biomass burning associated with the cosmic impact at the onset of Younger Dryas cooling (Firestone et al. 2007).

Aciniform Carbon

Description

"Soot" or "black carbon" refers primarily to elemental carbon components remaining after incomplete combustion. Soot includes all particulates collected above a flame in a fire, whereas aciniform carbon is a subcategory of soot. For YDB studies, the two terms are used interchangeably. Abundance peaks in aciniform carbon have previously been interpreted as definitive evidence for impact-related fires at the K-Pg impact boundary (Wolbach et al. 1985) and also serve as evidence for increased biomass burning at the time of the YDB impact event (Firestone et al. 2007).

Characteristics

The distinctive morphology of aciniform carbon enables quantification using scanning electron microscopy (SEM). Aciniform carbon consists of chainlike aggregates of 10–30 spherical units, each with diameters of 10–50 nm, arranged in necklace-like chains or "grape-like" aciniform clusters (Figure 8.2B) (Calcote 1981; Harris and Weiner 1985). In the YDB layer, typical sizes of aciniform carbon clusters are < 1 μm, ranging in abundance from ≈100 to 6,100 ppm and averaging ≈1,480 ppm (Firestone et al. 2007).

Preservation

Following deposition, aciniform carbon and soot are subject to relatively rapid oxidation, and consequently they are generally found only in sediments deposited under oxygen-deficient, reducing conditions. Soot is rarely found in sedimentary profiles, because its high surface-to-volume ratio results in rapid loss through oxidation over time. Soot was preserved globally at the K-Pg boundary, most likely because of rapid burial associated with the impact event, protecting it from oxidation. A similar, less intense burial process may have preserved aciniform carbon in the YDB layer at some sites.

Distribution

Aciniform carbon production is influenced by many variables, including fuel source, moisture levels, humidity, temperature, O2 availability, and CO2 concentrations above the fire. After formation, soot can be carried significant distances from the fire; hence, it is not necessarily an indicator of local fires. Aciniform carbon was found in the YDB layer at 7 of 15 sites tested across two continents (Firestone et al. 2007; Kennett et al. 2015).

Inconsistent Origins

(1) Cosmic origin: there is no reported evidence that aciniform carbon is delivered to Earth from space. (2) Anthropogenic origin: coal-fired power plants produce soot, but it is found in surface layers, whereas the YDB layer at most sites is buried and sealed >2 m below the surface, precluding migration of aciniform carbon downward. (3) Authigenic origin: aciniform carbon cannot be authigenically produced. (4) Volcanic origin: if trees are burned by an eruption, soot can be produced, but the YDB layers contain no tephra, ash, or geochemical anomalies related to volcanism. (5) Origin

by lightning: this process is precluded, because aciniform carbon and soot are nonmagnetic.

Impact-Related Origin

YDB aciniform carbon is found with other proxies known to be associated with impact events, and this association has never been found in sedimentary contexts that can be attributed to any other source besides an impact event. Based on SEM observations by one of us (Wolbach), soot from both the YDB and K-Pg layers exhibits similar morphology and particle size distribution (Wolbach et al. 1985). K-Pg soot was found globally at more than 12 widely dispersed sites (Wolbach et al. 1990; Wolbach et al. 2003), and similarly, YDB soot has been found at seven North American sites, consistent with production during a major cosmic impact event.

Formation

YDB aciniform carbon likely formed through extensive biomass burning at temperatures higher than those of typical wildfires. Initially, it may have resulted directly from the YDB airburst/impacts and then subsequently from burning of biomass that was decimated by rapid climate change. An impact into or over the ice sheet would have produced little aciniform carbon from biomass burning, but some may have formed from vaporization of carbon-rich target rocks (e.g., limestone) or hydrocarbons trapped in target rocks, as is proposed for the K-Pg event. (Kinzie et al. 2014 and references therein).

Carbon Spherules Containing Nanodiamonds

These small, distinctive, black carbonaceous spheres form from boiling tree sap and by condensation of high-temperature, carbon-rich vapor. They commonly range in size from .15 to 2.5 mm and have an average YDB abundance of ≈250/kg (Figure 8.3A) (Firestone et al. 2007; Israde et al. 2012; Kinzie et al. 2014). At 20 sites on four continents, YDB carbon spherules exhibit peak abundances in response to widespread biomass burning (Kennett et al. 2015). They are easily separated from sediment using sieves or flotation and are readily identified, given their relatively large size, often shiny, smooth surfaces, and distinctive honeycomb interior ultrastructure and outer crust (Firestone et al. 2007). This structure is readily observed using a regular stereoscopic light microscope, but especially by using SEM. Because carbon spherules peak in abundance in the YDB layer at many

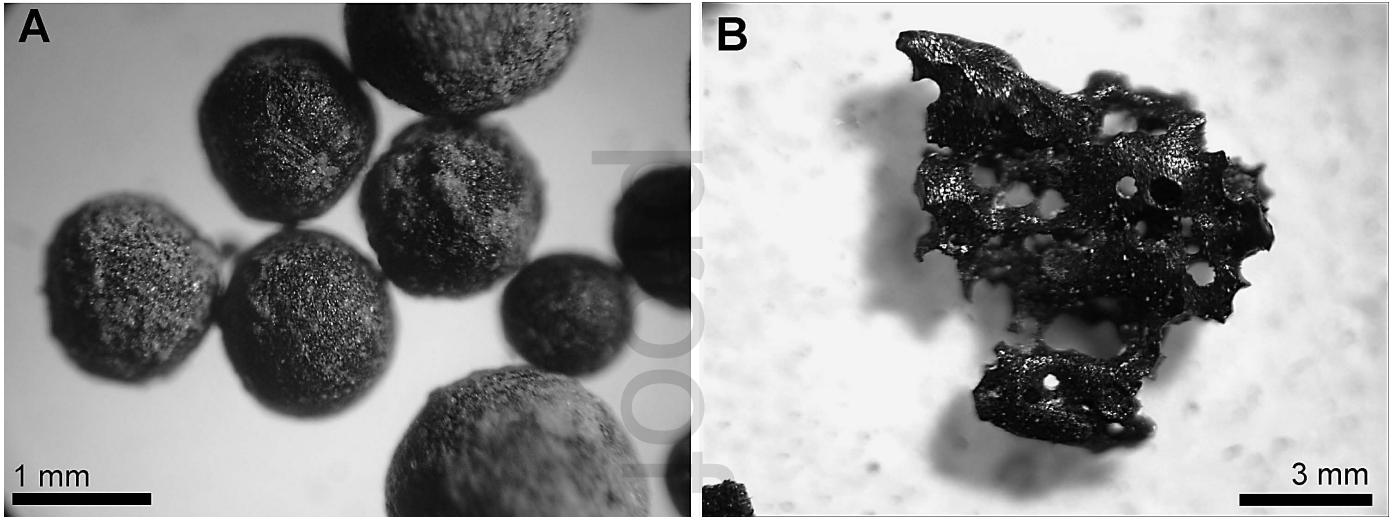

Figure 8.3. Photomicrographs of (A) carbon spherules from Gainey, Michigan, and (B) glass-like carbon from Santa Maira, Spain. Both of these materials from the YDB layer were found to contain nanodiamonds observed using high-resolution transmission electron microscopy.

sites, they are useful as a preliminary indicator of the location of the YDB layer prior to additional, more-detailed analyses for other proxies.

Carbon spherules are typically found in natural, high-temperature wildfires, so they are not uniquely diagnostic of an impact event. What makes YDB carbon spherules unusual is that they often contain nanodiamonds with the same characteristics as those found in sediments (see nanodiamond section above). Laboratory experiments indicate that these nanodiamond-rich carbon spherules require hypoxic atmospheres at 1,000 to 1,200 °*C*, conditions that do not exist in normal wildfires but occur during an impact event. Hence, those containing nanodiamonds most likely formed under high-temperature, hypoxic conditions at the time of the YDB impact.

Glass-Like Carbon Containing Nanodiamonds

These materials have the same composition as carbon spherules but lack the spherulitic shape and the honeycomb interior. Instead, these objects are composed of black, highly angular, smooth-textured carbon glass that can also exhibit conchoidal fracturing. They typically range in size from a few microns to several cm and average ≈1.0 g/kg (Figure 8.3B) (Firestone et al. 2007). As with carbon spherules, glass-like carbon forms from burning tree sap and can be common in all natural, high-temperature wildfires. What can be unique about this material when found in the YDB layer is that it can contain nanodiamonds, otherwise not found outside the layer at high concentrations.

Charcoal

Charcoal is a well-known product of natural wildfires and thus is not uniquely diagnostic of an impact event. However, the YDB layer at 20 synchronous sites on four continents contains a distinct abundance peak in charcoal (Kennett et al. 2015), indicating that fires were widespread and common at the time of the impact event, although some may represent human campfires. This pattern is also consistent with evidence from the K-Pg impact event (Firestone et al. 2007 and references therein). Charcoal in the YDB layer ranges in size from a few microns to several centimeters and exhibits average concentration values of 1.4 g/kg (Firestone et al. 2007).

Biomass Burning Processes at YDB

To produce the fire-related proxies observed to peak in the YDB layer in many locations, distal ejecta and secondary impacts would have ignited

scattered fires on land. Such fires would have been widespread, but there is no evidence, or necessity, that they were ubiquitous (Marlon et al. 2009). Wildfires induced directly by an impact's thermal pulse would instantly ignite beneath the fireball, but because of the curvature of the Earth, these would be limited by distance from the fireball. For example, an airburst ≈5 km above Earth's surface would be directly visible only ≈250 km away, and thus incapable of starting fires farther away. The intensity of thermal radiation declines exponentially with distance, and so, even at distances of < 250 km, thermally induced fires would have occurred only near the fireball. In addition, high-temperature ejecta would have been capable of igniting wildfires at greater distances.

If multiple YDB airbursts occurred, impact-related fires would have been intense and numerous, but widely separated. As recorded in the Greenland Ice Sheet, there is strong independent evidence of a major peak in biomass burning at the onset of the Younger Dryas. The concentrations of wildfire-related aerosols (NH4, NOx) represent the largest such episode in the previous 386,000 years, the temporal limit of the record (Kurbatov et al. 2011 and references therein). This represents unequivocal evidence for major biomass burning apparently coeval with a Younger Dryas impact event.

The estimate of the annual area burned by wildfires across one hemisphere is ≈2,000,000 km2 for one hemisphere, representing ≈2.7 percent of the land surface (Yang et al. 2014). Napier et al. (2013) speculated that the YDB impact event may have included ≈5,000 airbursts equal to or larger than the Tunguska airburst, which burned 500 km2 of forest. Although there are many variables, if that estimated number is correct, then up to 2,500,000 km2 could have burned in a single day, totaling ≈3 percent of Earth's surface. Thus, in just one day, such fires would have burned more area than all the current annual wildfires across one hemisphere, accounting for >300 times more biomass burning proxies at the Younger Dryas onset. It is also possible that the increase in biomass burning at the YDB resulted from an abundance of dead, dry biomass fuel. Major and abrupt environmental degradation resulting from the impact, in addition to abrupt cooling at the onset of the Younger Dryas, almost certainly would have been a major contributor to increased abundances of highly combustible fuel. Both these effects, high-temperature airbursts and combustible fuel, are proposed to have occurred over broad areas of Earth and could explain the wide distribution of evidence for biomass burning at the YDB.

Characteristics of the Younger Dryas Impact(s)

At present, there is insufficient evidence to determine the characteristics of the YDB impactor(s), but there are a number of clues. Here, we provide a brief overview of several possibilities that have previously been proposed.

What was it? Firestone et al. (2007) speculated that because YDB proxies are carbon-enriched and nickel-depleted, the impactor most likely was a comet, either fragmented or whole. Alternately, Petaev et al. (2013) discovered YDB platinum enrichment in an ice core recovered by the Greenland Ice Core Project (GISP2), leading them to suggest that the YDB impactor was an iron-rich, iridium-depleted iron meteorite. Offering a comet-related explanation, Napier et al. (2013) proposed that the Younger Dryas impact resulted from a comet swarm of sufficient size and magnitude to deposit widespread proxies, ignite wildfires, and cause megafaunal extinctions (Napier 2010). They noted that giant comets, called centaurs, enter Earth-crossing orbits approximately every 175,000 years, with each episode lasting a few thousand years (Napier et al. 2013). One of the largest centaurs, Chiron, is more than 200 km in diameter and currently orbits beyond Saturn. Such objects are known to undergo hierarchic disintegrations, during which multiple collisions with Earth are possible (Napier et al. 2015). *What size was it?* For impacts in general, Toon et al. (1997), as cited in Firestone et al. (2007), concluded that an impact capable of continent-wide damage requires an impact by a comet that is >4 km wide. Previously, Chapman and Morrison (1994) loosely estimated an even lower threshold by predicting widespread catastrophes for impactors ranging from 500 m to 5 km. Pierazzo and Artemieva (2012) calculated that a 1-km to 10-km impactor would cause a global catastrophe, injecting enough dust into the stratosphere to alter climate, cause mass starvation, and trigger widespread epidemics. Pierazzo et al. (2010) reported model results indicating that an oceanic impact by a 1-km asteroid or comet could inject enough water vapor and aerosols to diminish ozone production for a period of years. More intense impacts produce greater vapor plume heights, corresponding to proportionally greater ozone destruction. This depletion would allow harmful levels of UVB radiation to reach Earth's surface, with potentially catastrophic consequences for terrestrial and marine ecosystems, possibly contributing to extinctions. A similarly sized object impacting a large continental ice sheet should have similar consequences.

For the Younger Dryas impact event, Firestone et al. (2007) suggested

that the impactor originally had a diameter larger than 4 km. They proposed that before impacting Earth, the comet broke up in space (not Earth's atmosphere) to produce a comet swarm of unknown mass, but with some fragments as large as ≈2 km in diameter. In addition, multiple smaller fragments would have exploded as atmospheric airbursts, as occurred at Tunguska, Siberia, in 1908. Israde et al. (2012) suggested that the impactor was a fragmented object that originally was larger than several hundred meters in diameter.

As proposed by Napier et al. (2013), if the YDB cometary fragments equaled one-thousandth the mass of 200-km-wide centaur Chiron (that is, a fragment equivalent to a 20-km-wide object), those fragments could have produced ≈5,000 catastrophic, Tunguska-sized airburst/impacts over one hemisphere of the Earth within just a few hours.

Where did the impact occur? Based on the geographic distribution and concentration of proxies, along with the current lack of obvious YDB craters, Firestone et al. (2007) concluded that the largest of the comet fragments struck glaciated portions of eastern Canada. Those authors cited NASA experiments showing that multiple 2-km cometary fragments could have impacted the Laurentide Ice Sheet (up to ≈3 km thick), leaving shallow or no craters. In support of that, the Tunguska event and the Dakhleh event show that devastating airbursts can occur without leaving a visible crater (Firestone et al. 2007; Napier et al. 2013). The calculations of Napier et al. (2013) suggest that a highly devastating comet swarm could have occurred over one hemisphere of the planet without producing craters.

Conclusions

Of all the possible mechanisms that could account for the diverse assemblage of YDB proxies found variably at 32 sites on four continents, only a cosmic impact event could have produced all of them together. The ages of 22 YDB sites on four continents are statistically isochronous, within the limits of dating methodologies, indicating that a temporally singular impact event occurred, affecting at least one hemisphere. The evidence suggests that the impact event was environmentally catastrophic, abruptly changing ocean circulation, triggering severe Younger Dryas climate change, contributing to megafaunal extinctions, and causing human cultural shifts and population declines in people and animals, as discussed in a companion chapter in this volume.